Optimization of the CMB-galaxy cross-correlation signal for studying the Integrated Sachs-Wolfe effect

Arthur Diniz Meirelles

Advisor: Edivaldo Moura Santos
Coadvisor: Ronaldo Carloto Batista

Institute of Physics
Universidade de São Paulo

15/08/2024

1 Theoretical Aspects

2 Optimized Galaxy Survey

3 Data Processing

4 Analysis and Results

5 Conclusions

1 Theoretical Aspects

2 Optimized Galaxy Survey

3 Data Processing

4 Analysis and Results

5 Conclusions

Introduction

- The integrated Sachs-Wolfe (ISW) effect occurs due to time changes in gravitational potentials;

- During periods of transition from or to matter-dominated eras of the Universe, potentials change more rapidly;

- Naturally, a statistical correlation between CMB temperature maps and gravitational potentials is expected.
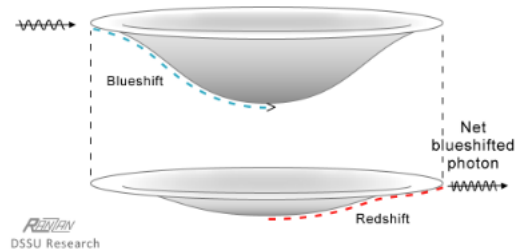

Figure 2: Illustration of the ISW effect. In this case, the gravity wells flattened, leaving a net blueshift.

The ΛCDM Model

To build the theoretical framework used, it is assumed

- The Universe is homogeneous and isotropic at large scales;
- Initial conditions are obtained by assuming an inflationary period when the Universe was very compact and energetic;
- The Universe is composed of baryonic matter, radiation, neutrinos, cold dark matter and a dark energy component described by a cosmological constant Λ;
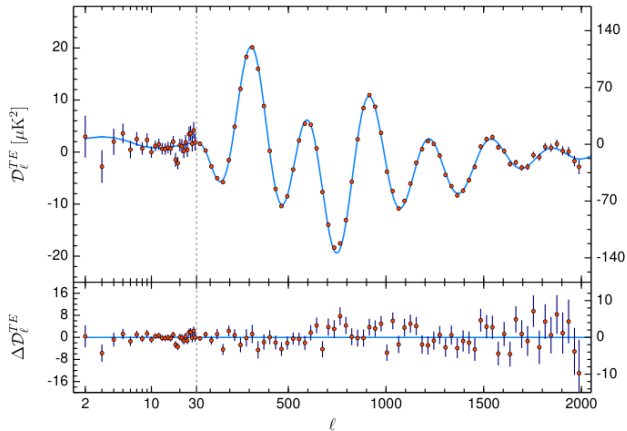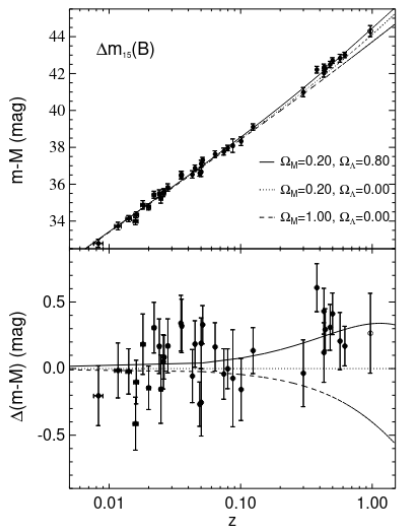
The homogeneous and isotropic background is first set up, and linear perturbations are added to it.

The Perturbed Metric

We express the perturbed metric with two functions $\Psi(\mathbf{x}, t)$ and $\Phi(\mathbf{x}, t)$

$$\begin{cases} g_{00} = -1 - 2\Psi(\mathbf{x}, t), \\ g_{0i} = g_{i0} = 0, \\ g_{ij} = a^2(t)\delta_{ij}[1 + 2\Phi(\mathbf{x}, t)]. \end{cases} \tag{1}$$

The ΛCDM Model

The Cosmic Microwave Background

The temperature of the Cosmic Microwave Background (CMB) can be expressed by

$$T(\mathbf{x}, \hat{\mathbf{p}}, t) = \bar{T}(t)[1 + \Theta(\mathbf{x}, \hat{\mathbf{p}}, t)]. \tag{2}$$

The temperature perturbation Θ can be expressed in Fourier space according to

$$\Theta(\hat{\mathbf{k}}, \mu) = \sum_{\ell=0}^{\infty} (2\ell + 1)(-i)^{\ell} \Theta_{\ell}(\hat{\mathbf{k}}) \mathscr{P}_{\ell}(\mu), \tag{3}$$

where $\mu = \hat{\mathbf{k}} \cdot \hat{\mathbf{p}}$ and $\mathscr{P}_{\ell}$ are Legendre polynomials.

Analytical Approximation

Working with first-order equations and the tightly coupled limit, and assuming recombination to be an instantaneous process happening at conformal time $\eta = \eta*$, we can obtain

$$\begin{aligned}
\Theta_\ell(k, \eta_0) \approx &[\Theta_0(k, \eta_*) + \Psi(k, \eta_*)] j_\ell[k(\eta_0 - \eta_*)] \\
&+ iv_b(k, \eta_*) \left\{ j_\ell[k(\eta_0 - \eta_*)] - (\ell + 1) \frac{j_\ell[k(\eta_0 - \eta_*)]}{k(\eta_0 - \eta_*)} \right\} \\
&+ \int_0^{\eta_0} d\eta e^{-\tau} [\Psi'(k, \eta) - \Phi'(k, \eta)] j_\ell[k(\eta_0 - \eta)].
\end{aligned} \tag{4}$$

Here, the third term in the equation describes the Integrated Sachs-Wolfe effect.

Correlation Functions

To calculate the CMB autocorrelation function C_ℓ^{tt}, we expand Θ in spherical harmonics

$$\Theta(\mathbf{x}, \hat{\mathbf{p}}, t) = \sum_{\ell=1}^{\ell_{max}} \sum_{m=-\ell}^{\ell} a_{\ell m}(\mathbf{x}, t) \, Y_{\ell m}(\hat{\mathbf{p}}), \tag{5}$$

and calculate the autocorrelation between the $a_{\ell m}$ terms:

$$\langle a_{\ell m} a_{\ell' m'}^* \rangle = \delta_{\ell \ell'} \delta_{mm'} C_\ell^{tt} \tag{6}$$

Other autocorrelation spectra C_ℓ^{xx} follow the same process. It is common to use $D_\ell^{XX} = \frac{\ell(\ell+1)}{2\pi} C_\ell^{xx}$ for some spectra for better visualization. We can also write

$$`C_\ell^{tt} = \frac{1}{2\ell+1} \sum_{m=-\ell}^{\ell} a_{\ell m} a_{\ell' m'}^* \tag{7}$$

Cosmic Variance

The low number of $a_{\ell m}$ coefficients for lower multipoles ℓ leads to a high uncertainty in this region called cosmic variance

$$\left(\frac{\Delta C_\ell^{XX}}{C_\ell^{XX}}\right)_{CV} = \sqrt{\frac{2}{2\ell + 1}} \tag{8}$$

Planck 2018

Figure 3: Planck 2018 CMB temperature power spectrum.

Parameter	Best-fit
$\Omega_b h^2$	0.02237 ± 0.00015
$\Omega_c h^2$	0.1200 ± 0.0012
$100\Theta_{MC}$	1.04092 ± 0.00031
τ	0.0544 ± 0.0073
$\ln(10^{10} A_s)$	3.044 ± 0.014
n_s	0.9649 ± 0.042
Ω_m	0.3153 ± 0.0073
H_0	$67.36 \pm 0.54 \ \mathrm{km/s/Mpc}$
σ_8	0.8111 ± 0.0060

Table 1: Best-fit values of cosmological parameters reported in Planck 2018 results using TT+TE+EE+lowE and gravitational lensing data.

The Matter Power Spectrum

To calculate a cross-correlation function, we need the 3D matter power spectrum $P(k, z)$, defined by

$$\left\langle \delta(\mathbf{k}, z)\delta^*(\mathbf{k}', z) \right\rangle = (2\pi)^3 P(k, z)\delta_D(\mathbf{k} - \mathbf{k}')$$

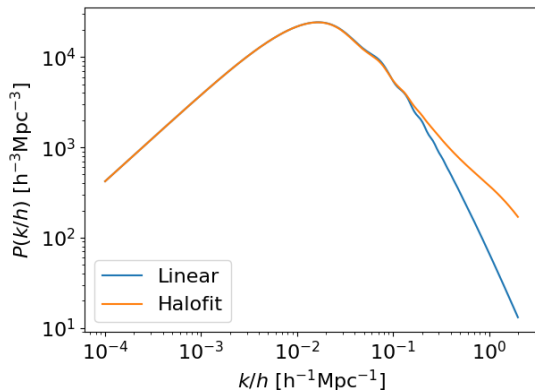We have used CAMB's implementation of the HALOFIT model to calculate the matter power spectrum.

Figure 4: Matter power spectrum calculated using both a linear approximation and the HALOFIT model.

The Cross-correlation Spectrum

To trace the matter density anisotropies, we used galaxy contrast maps, which can be calculated using

$$\delta_g(\mathbf{n}) = \frac{N_g(\mathbf{n}) - \bar{N}_g}{\bar{N}_g} \tag{9}$$

It is assumed that $\delta_g = b_g \delta$, where b_g is the bias factor, which we assume to be a slowly varying function of redshift.

The galaxy autocorrelation C_ℓ^{gg} and cross-correlation function C_ℓ^{tg} can then be calculated with

$$\langle a_{\ell m}^t a_{\ell' m'}^g \rangle = C_\ell^{tg} \delta_{\ell \ell'} \delta_{mm'} \qquad\qquad \langle a_{\ell m}^g a_{\ell' m'}^g \rangle = C_\ell^{gg} \delta_{\ell \ell'} \delta_{mm'} \tag{10}$$

Analytical Formula

Given fields x and y, representing either the ISW contribution to the CMB temperature ($x, y = t$) or the galaxy contrast ($x, y = g$), we can calculate the associated auto- or cross-correlation spectra using [1]

$$C_\ell^{xy} = \frac{2}{\pi} \int dk k^2 W_\ell^x(k) W_\ell^y(k) P(k), \tag{11}$$

with

$$W_\ell^t = -3\Omega_m \left(\frac{H_0}{k}\right)^2 \int dz \frac{d[(1+z)D(z)]}{dz} j_\ell[k\chi(z)] \tag{12}$$

$$W_\ell^g = \int dz b_g(z) \frac{dN}{dz} D(z) j_\ell[k\chi(z)] \tag{13}$$

ISW Contribution: Temperature Autocorrelation
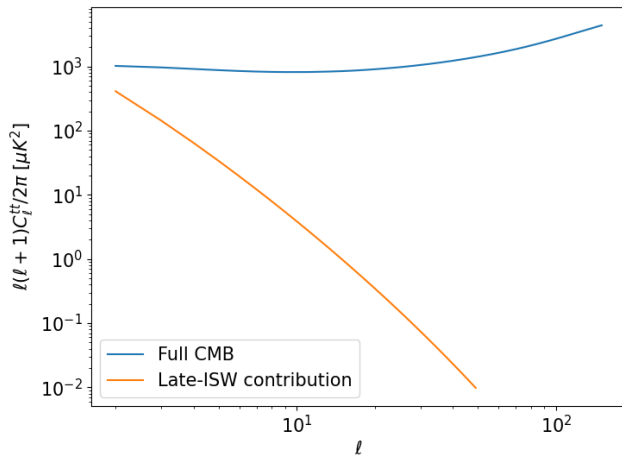
Figure 5: CMB autocorrelation comparison between full spectrum and ISW contribution.

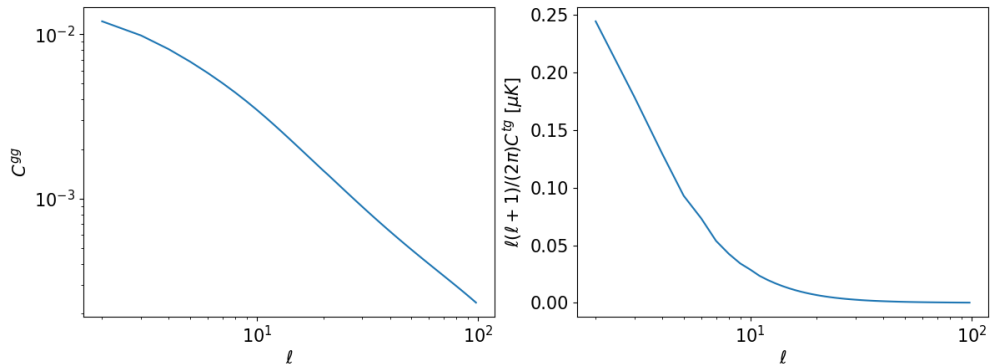## ISW Contribution: Galaxy Autocorrelation and Cross-correlation

Figure 6: Galaxy autocorrelation spectrum (left) and late-ISW contribution to the galaxy-CMB cross-correlation (right).

1 Theoretical Aspects

2 Optimized Galaxy Survey

3 Data Processing

4 Analysis and Results

5 Conclusions

Selection Function Parametrization

The function $\frac{dN}{dz}$ in equation (13) is called the selection function. We are assuming its parametrization to be [2]

$$\frac{dN}{dz}\left(z|\lambda, \beta, z_0\right) dz = \frac{\beta}{\Gamma(\lambda)} \left(\frac{z}{z_0}\right)^{\beta\lambda-1} \exp\left[-\left(\frac{z}{z_0}\right)^{\beta}\right] d\left(\frac{z}{z_0}\right) \tag{14}$$

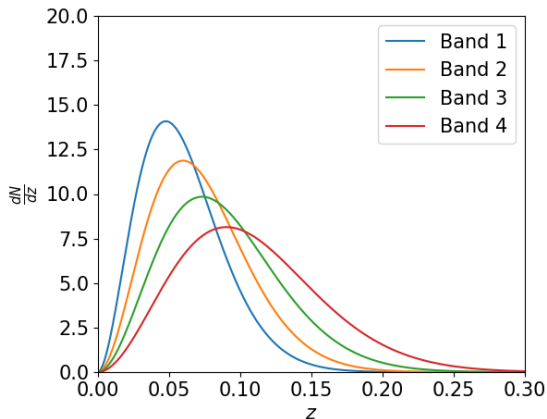We have explored how to maximize the cross-correlation signal using an idealized selection function.

2MASS Bands Comparison

Figure 7: Selection function calculated for the 4 bands of the 2MASS catalog.

Band	z_0	β	λ
1	0.043	1.825	1.524
2	0.054	1.800	1.600
3	0.067	1.765	1.636
4	0.084	1.723	1.684

Table 2: Parameter values for the 4 bands of the 2MASS catalog.
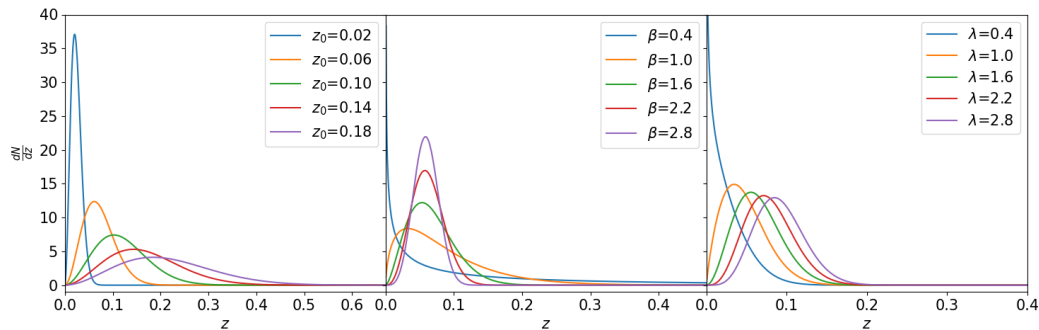
Exploring the Parameter Space

Figure 8: Selection function calculated for various parameter values.

Null Hypothesis

For the process of finding a galaxy survey with an idealized selection function, we first needed an estimation for the probability of C_ℓ^{tg} being 0, which would be our null hypothesis. The following process was used:

- Synthesize multiple uncorrelated CMB temperature and galaxy contrast maps using HEALPix;
- Calculate the cross-correlation C_ℓ^{tg} for each pair of uncorrelated maps at each multipole;
- For each multipole ℓ, a histogram of C_ℓ^{tg} was produced;
- Each histogram was fit with Gaussian distributions with average $\mu = \mu_\ell \approx 0$ and $\sigma^2 = \sigma_\ell^2$.

The null hypothesis is compatible with $\Omega_m = 1$.

Synthesized Maps' Histograms
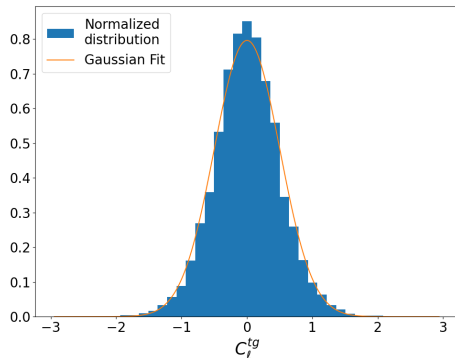
(a) $\ell = 4$
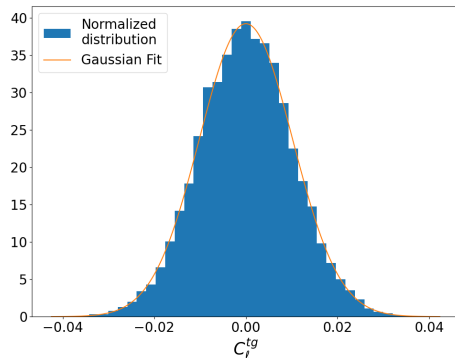
(b) $\ell = 30$

Figure 9: Distribution of cross-correlation values on different multipoles for 10^4 maps synthesized with null cross-correlation.

Null Hypothesis

For f_ℓ corresponding to the Gaussian fit made for the multipole ℓ

$$f_\ell(C_\ell^{tg}) = \frac{1}{\sqrt{2\pi\sigma_\ell^2}} \exp\left[-\frac{1}{2}\left(\frac{C_\ell^{tg} - \mu_\ell}{\sigma_\ell}\right)^2\right], \tag{15}$$

we have defined the null hypothesis probability distribution to be

$$P_{\text{null}} = \prod_{\ell=2}^{\ell_{\max}} f_\ell(C_\ell^{tg}) \tag{16}$$

Exploring the Parameter Space

For various points (β, z_0, λ) in the parameter space, we have calculated the ratio $P_{\text{null}}(\beta, z_0, \lambda) / P_{\text{null}}^{\text{2MASS}}$ and produced the heat maps in Figure 10.
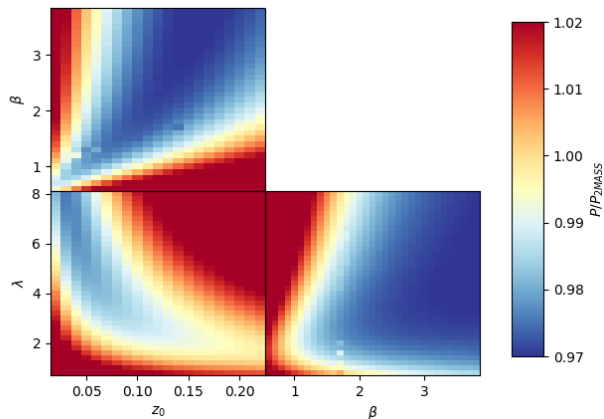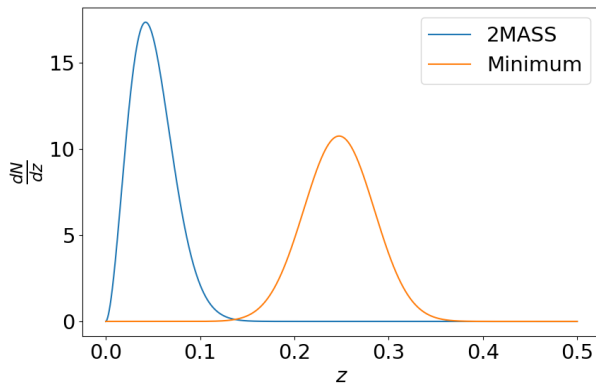

Figure 10: Heat maps used to explore the parameter space.

Minimizer

The heat maps provided initial points to run an algorithm that minimizes $P_{\mathrm{null}}(z_0, \beta, \lambda)$. The point found that minimizes the null hypothesis probability in that region of the parameter space was

$$(\beta, z_0, \lambda) = (3.088, 0.1508, 4.9401) \tag{17}$$

Properties of the Minimum

The selection function found is deeper than that of 2MASS band 1. It does not favor galaxies at $z^* = 0.63$, the estimated redshift at which the accelerated expansion started.

Figure 11: Selection functions comparison.

Properties of the Minimum

The selection function found reduces the maximum value of the cross-correlation function, but its peak is at higher redshifts ($\ell \approx 10$), reducing the influence of cosmic variance in the signal.
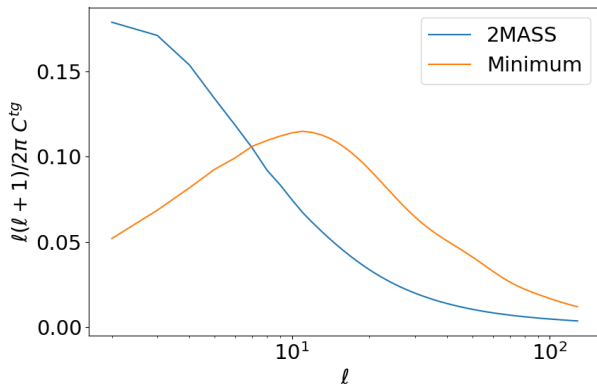

Figure 12: Theoretical cross-correlation spectrum comparison.

Discussion

- The ratio $P_{\text{null}}(z_0, \beta, \lambda) / P_{\text{null}}^{2\text{MASS}} = 0.971$ for the minimum;
- Despite the small statistical gain, this optimal selection function yields reasonably better results for constraints on Ω_m, as will be discussed;
- A similar work has reported a small preference towards the non-null signal with changes to the depth of the survey and fainter magnitude limits [3].

1 Theoretical Aspects

2 Optimized Galaxy Survey

3 Data Processing

4 Analysis and Results

5 Conclusions

WMAP Data

The CMB temperature maps used in this project are the ones provided by WMAP9 [4].

- Three frequency bands were used, which are named bands Q (40GHz), V (60GHz) and W (90GHz);
- The temperature intensity maps' noise power can be well modeled as uncorrelated Gaussian fluctuations;
- Despite having a lower resolution (0.3°) compared to Planck's (0.083°), this project focuses on lower multipoles;
- We have combined both maps' masks and used it for analysing each one, resulting in a fraction $f_{sky} = 0.7$.

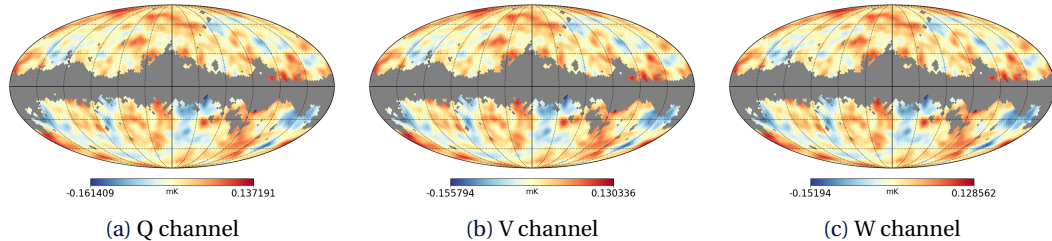## WMAP Data

(a) Q channel

(b) V channel

(c) W channel

Figure 13: Mollweide projection of three (Q, V, W) WMAP9 CMB temperature (in mK) maps in galactic coordinates with an $f_{\text{sky}} = 0.70$ mask applied
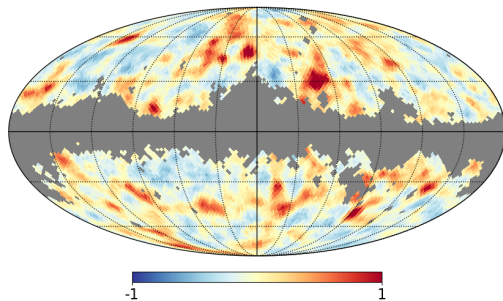
2MASS Catalog

Wide sky coverage is a very influential aspect of studying cross-correlation spectra, and the 2MASS catalog contains raw imaging data covering 99.998% of the sky [5], which was the dataset used.

- We have used the K_s ($2.16\,\mu$m) band of the Extended Source Catalog (XSC);
- The data of the K_s band obtained from a 20 mag aperture (K_{20}) were corrected for galactic extinction, and the remaining data was further divided into 4 bands: Bands 1 ($12.0 < K'_{20} < 12.5$), 2 ($12.5 < K'_{20} < 13.0$), 3 ($13.0 < K'_{20} < 13.5$) and 4 ($13.5 < K'_{20} < 14.0$);
- Each band has a different selection function, as shown in Figure 7.
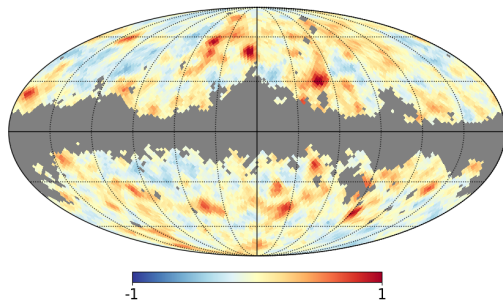
2MASS Catalog
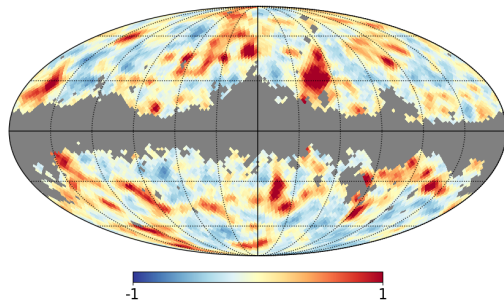
(a) Band 1   (b) Band 2

Figure 14: Mollweide projection of the 2MASS-XSC galaxy contrast maps in galactic coordinates with the combined 2MASS+WMAP mask applied ($f_{sky} = 0.70$).
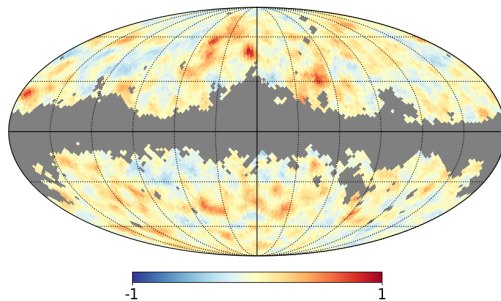
2MASS Catalog

(a) Band 3   (b) Band 4

Figure 15: Mollweide projection of the 2MASS-XSC galaxy contrast maps in galactic coordinates with the combined 2MASS+WMAP mask applied ($f_{sky} = 0.70$).

Correlation Spectra Estimator

To estimate the correlation spectra that describe the pixelized maps d with primordial signal s and noise n (with $\mathbf{S}$ and $\mathbf{N}$ being the corresponding covariance matrices), we could use the following likelihood function.

$$\mathscr{L} = P(\mathbf{d}|\mathbf{C}) = \frac{1}{(2\pi)^{n_{\dim}/2}|\mathbf{C}|^{1/2}} \exp\left(-\frac{1}{2}\mathbf{d}^T\mathbf{C}^{-1}\mathbf{d}\right), \qquad \mathbf{C} = \mathbf{S} + \mathbf{N} \qquad (18)$$

With a prior $\pi(\mathbf{S})$ we can use Bayes' Theorem to obtain

$$P(\mathbf{C}|\mathbf{d}) \propto \pi(\mathbf{S})P(\mathbf{d}|\mathbf{C}) \qquad (19)$$

Correlation Spectra Estimator

If we can sample from $P(\mathbf{C}|\mathbf{s}, d)$ and $P(\mathbf{s}|\mathbf{C}, d)$. Then we iterate

$$\mathbf{s}^{i+1} \leftarrow P(\mathbf{s}|\mathbf{C}^i, d) \tag{20}$$

$$\mathbf{C}^{i+1} \leftarrow P(\mathbf{C}|\mathbf{s}^{i+1}, d), \tag{21}$$

to obtain a sample of $\{(\mathbf{s}^i, \mathbf{C}^i)\}$.

The Blackwell-Rao Estimator

We can then use the Blackwell-Rao estimator to obtain an approximation for $P(C_\ell|\mathbf{d})$

$$P(C_\ell|\mathbf{d}) \approx \frac{1}{N_G} \sum_{i=1}^{N_G} P(C_\ell|\sigma_\ell^i), \tag{22}$$

where

$$\sigma_\ell^i = \frac{1}{2\ell+1} \sum_{m=-\ell}^{\ell} \mathbf{s}_{\ell m} \mathbf{s}_{\ell m}^\dagger. \tag{23}$$

We then maximize the probability $P(C_\ell|\mathbf{d})$ to obtain the best-fit C_ℓ.

Matrices Used

In this work, **s** and **S** are defined by

$$\mathbf{s}^T = (s_{00}^{tg}, s_{01}^{tg}, s_{11}^{tg}, \ldots, s_{\ell_{\max}0}^{tg}, \ldots, s_{\ell_{\max}\ell_{\max}}^{tg}), \tag{24}$$

$$\mathbf{S} = \mathrm{diag}(S_0^{tg}, S_1^{tg}, S_1^{tg}, \ldots, S_{\ell_{\max}}^{tg}, \ldots, S_{\ell_{\max}}^{tg}), \tag{25}$$

where

$$\mathbf{s}_{\ell m}^{tg} = \begin{pmatrix} a_{\ell m}^t \\ a_{\ell m}^g \end{pmatrix}, \qquad\qquad \mathbf{S}_\ell^{tg} = \begin{pmatrix} C_\ell^{tt} & C_\ell^{tg} \\ C_\ell^{tg} & C_\ell^{gg} \end{pmatrix}. \tag{26}$$

Correlation Spectra Obtained
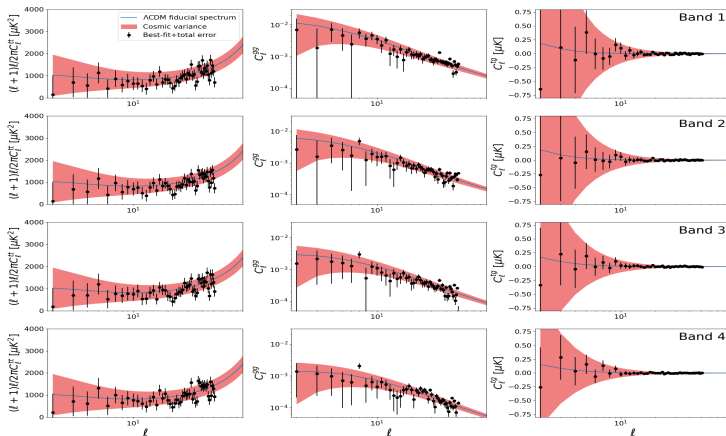

Figure 16: Comparison between theoretical correlation spectra and the ones estimated from WMAP and 2MASS.

1 Theoretical Aspects

2 Optimized Galaxy Survey

3 Data Processing

4 Analysis and Results

5 Conclusions

Monte Carlo Markov Chains

By defining the likelihood $\mathcal{L}(C_\ell|\theta)$ and the prior $p(\theta)$, one can use Markov chains to obtain samples of each parameter in θ following the posterior

$$P(\theta|C_\ell) = \mathcal{L}(C_\ell|\theta)\,p(\theta) \tag{27}$$

Joint posteriors can be easily obtained from each parameter sample, strongly simplifying data analysis for multiple parameter models.
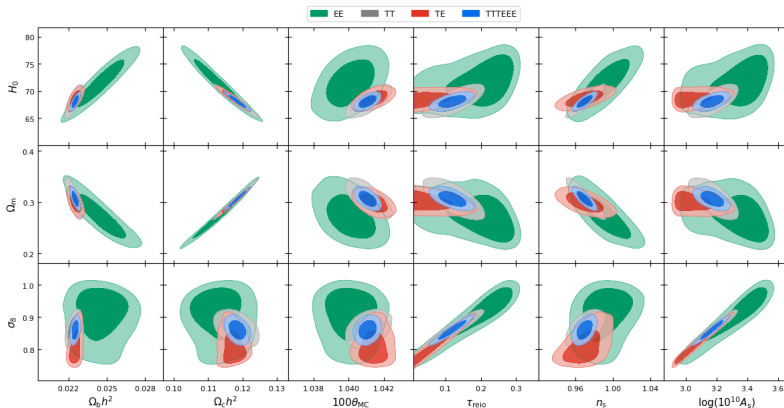
Planck Likelihoods

Figure 17: Joint posterior distributions of cosmological parameters using Planck's CMB temperature (T) and polarization (E) data.

Likelihood Profiling

The likelihood of each point in the spectrum was assumed to be Gaussian

$$\mathscr{L}(C_{\ell,\,\text{theo}}^{xy}|C_{\ell,\,\text{data}}^{xy}) = \frac{1}{\sigma_\ell \sqrt{2\pi}} \exp\left[-\frac{1}{2}\left(\frac{C_{\ell,\,\text{data}}^{xy} - C_{\ell,\,\text{theo}}^{xy}}{\sigma_\ell} \right)^2 \right]. \tag{28}$$
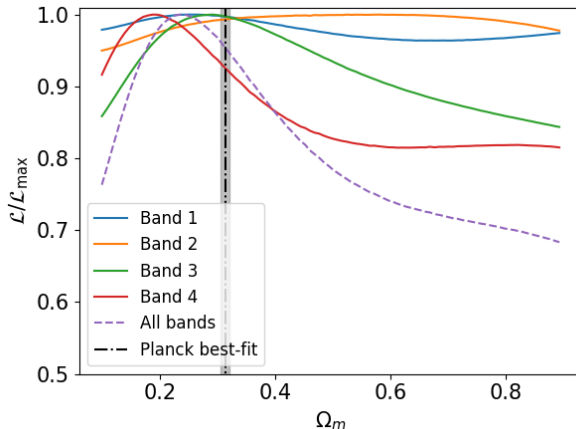
We are varying only Ω_m, so $C_{\ell,\,\text{theo}}^{xy}$ is a functions of only Ω_m. The likelihood of a full spectrum is

$$\mathscr{L}(\Omega_m|C_{\text{data}}^{xy}) = \prod_{\ell=2}^{\ell_{\max}} \mathscr{L}(C_{\ell,\,\text{theo}}^{xy}|C_{\ell,\,\text{data}}^{xy}). \tag{29}$$

The $C^{tg} + C^{gg}$ joint-likelihood is

$$\mathscr{L}(\Omega_m|C_{\text{data}}^{tg}, C_{\text{data}}^{gg}) = \mathscr{L}(\Omega_m|C_{\text{data}}^{tg})\mathscr{L}(\Omega_m|C_{\text{data}}^{gg}). \tag{30}$$
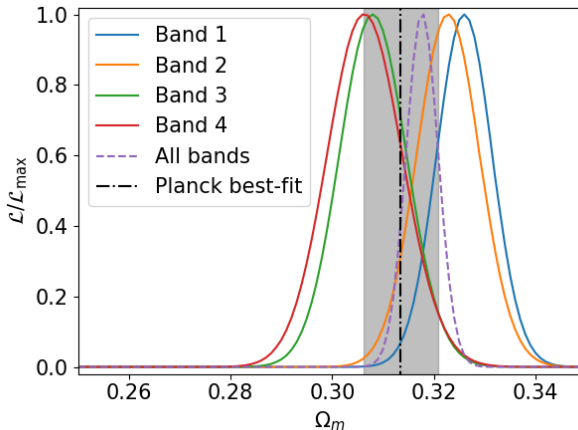
Results for 2MASS

- All curves are compatible with Planck;
- Not much constraining power on Ω_m;
- Bands 3 and 4 – which have the deepest selection functions – have the most constraining power amongst all 4.

Figure 18: C^{tg} only likelihood profiles.

Results for 2MASS

- All likelihoods are compatible with Planck;
- Very high constraining power on Ω_m when C^{gg} is introduced, comparable to Planck's;
- No significant difference in constraining power between each band.

Figure 19: Joint likelihood profiles

Forecast for the Optimized Band

To estimate the behavior of a survey that follows our idealized selection function in this analysis, we have produced two synthetic cross-correlation spectra using that selection function. Both use the ΛCDM model with Planck's best-fit parameters, only differing in Ω_m:

- One of the datasets was produced using Plancks best-fit of $\Omega_m = 0.3153$;
- The other dataset was produced using $\Omega_m = 0.188$, the value that maximizes the likelihood of band 4 for the C^{tg} only likelihood.

Band 4's errors were used as estimated for both synthetic datasets.

Forecast for the Optimized Band

Figure 20: Optimized band C^{tg} only profile.
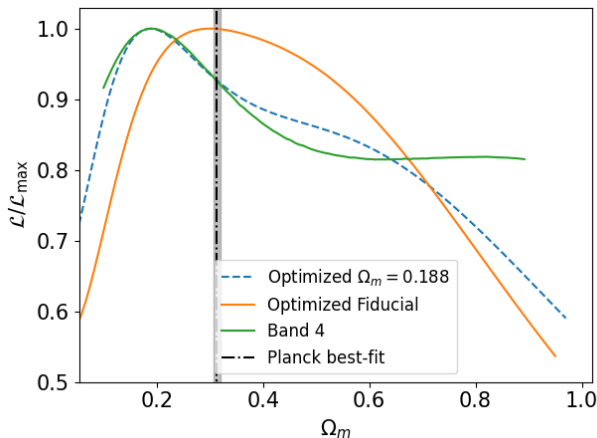
- Constraining power still low;
- Reasonable improvement in the constraining power.

Discussion

- The optimized band being deeper than 2MASS means errors on the spectra should be lower, meaning the errors used are overestimated, which indicates the constraints could be better for a real survey following our optimized selection function;

- The optimized band was not found by optimizing the Ω_m constraints, but rejecting the null cross-correlation hypothesis. $\Omega_m = 1$ leads to $C_\ell^{tg} = 0$, and the fast decrease in likelihood for higher Ω_m is noticeable.

1. Theoretical Aspects

2. Optimized Galaxy Survey

3. Data Processing

4. Analysis and Results

5. Conclusions

Conclusions

- We have obtained the likelihood profiles for Ω_m obtained from cross-correlation data by studying the ISW effect;

- The constraints obtained using only C^{tg} were not strong, but can be used as a complement to other datasets for a combined analysis;

- In the 2MASS catalog, the 2 deepest bands – bands 3 and 4 – yielded better constraining power;

- The Planck collaboration also studied the ISW effect using the cross-correlation spectrum[6], obtaining significantly better results with deeper surveys (SDSS[7] and Planck's Kappa map).

Conclusions

- An optimized band capable of maximizing the ISW signal was obtained, prioritizing galaxies at higher redshifts and increasing the cross-correlation signal in a region less affected by cosmic variance;
- The likelihoods obtained for artificial data calculated using the optimized band improved the constraints on Ω_m;
- Combining different matter tracers leads to improved results overall.

Theoretical Aspects
○○○○○○○○○○○○○○○○○

Optimized Galaxy Survey
○○○○○○○○○○○○○

Data Processing
○○○○○○○○○○○○○

Analysis and Results
○○○○○○○○○○

Conclusions
○○○●

Extras
○○

References

Thank You

Extra Content

Discussão de Future prospects

Extra Content

More extras

Bibliography I

[1] E. Moura-Santos et al. "A Bayesian Estimate of the CMB–large-scale Structure Cross-correlation". In: *The Astrophysical Journal* 826.2 (July 2016), p. 121. DOI: 10.3847/0004-637X/826/2/121. URL: https://dx.doi.org/10.3847/0004-637X/826/2/121.

[2] Niayesh Afshordi, Yeong-Shang Loh, and Michael A. Strauss. "Cross-correlation of the cosmic microwave background with the 2MASS galaxy survey: Signatures of dark energy, hot gas, and point sources". In: *Phys. Rev. D* 69 (8 Apr. 2004), p. 083524. DOI: 10.1103/PhysRevD.69.083524. URL: https://link.aps.org/doi/10.1103/PhysRevD.69.083524.

Bibliography II

[3] Caroline L. Francis and John A. Peacock. "Integrated Sachs–Wolfe measurements with photometric redshift surveys: 2MASS results and future prospects". In: *Monthly Notices of the Royal Astronomical Society* 406.1 (July 2010), pp. 2–13. ISSN: 0035-8711. DOI: 10.1111/j.1365-2966.2010.16278.x. eprint: https://academic.oup.com/mnras/article-pdf/406/1/2/3673745/mnras0406-0002.pdf. URL: https://doi.org/10.1111/j.1365-2966.2010.16278.x.

[4] M. R. Greason et al. *Wilkinson Microwave Anisotropy Probe (WMAP): Nine-Year Explanatory Supplement.* Available in electronic form at http://lambda.gsfc.nasa.gov/. NASA/GSFC. Greenbelt, MD, 2012.

[5] M. F. Skrutskie et al. "The Two Micron All Sky Survey (2MASS)". In: *The Astronomical Journal* 131.2 (Feb. 2006), p. 1163. DOI: 10.1086/498708. URL: https://dx.doi.org/10.1086/498708.

Bibliography III

[6] Planck Collaboration et al. "Planck 2015 results - XXI. The integrated Sachs-Wolfe effect". In: *A&A* 594 (2016), A21. DOI: 10.1051/0004-6361/201525831. URL: https://doi.org/10.1051/0004-6361/201525831.

[7] J. J. Condon et al. "The NRAO VLA Sky Survey". In: *The Astronomical Journal* 115.5 (May 1998), p. 1693. DOI: 10.1086/300337. URL: https://dx.doi.org/10.1086/300337.